

# Generalized Code Index Modulation Technique for High Data Rate Communication Systems

Georges Kaddoum, Yogesh Nijsure and Hung Tran

**Abstract**—In this paper, we propose a generalized code index modulation (CIM) technique for direct sequence-spread spectrum (DS-SS) communication. In particular, at the transmitter, the bit stream is divided into blocks in which each block is divided into two sub-blocks, named as mapped and modulated sub-block. Thereafter, the bits within the mapped sub-block are used to select one of the predefined spreading codes, which is then used to spread the modulated bits of the second sub-block. In this design, the use of the spreading code index as an information-bearing unit increases the overall spectral efficiency of this system. At the receiver side, the spreading code index is first estimated, thus resulting in a direct estimation of mapped sub-block bits. Consequently, the corresponding spreading code to this estimated index is used to de-spread the modulated symbol of the modulated sub-block. Subsequently, mathematical expressions for bit error rate, symbol error rate, throughput, energy efficiency, and the system complexity are derived to analyze the system performance. Finally, simulation results show that the proposed modulation scheme can achieve higher data rate than the conventional DS-SS system, with lower energy consumption and complexity.

**Index Terms**—Modulation, High Data Rate, Energy Efficiency, Performance Analysis, CIM.

## I. INTRODUCTION

The increasing number of network devices and wireless services in the last few years has resulted in an escalating demand for higher data rate. However, there exists a fact that the outburst of wireless devices and their energy consumption do not only cause serious negative effects to the environment (e.g. carbon footprint) but also brings up economic issues (e.g. power for a large number of base stations) for network operators. Recently, low energy consumption techniques for wireless technologies such as wireless body area networks (WBANs), wireless sensor networks (WSNs), internet of things (IoT), and satellite communications have been implemented widely as how to prolong the battery lifetime of wireless devices, as this issue becomes more serious [1–5]. All the aforementioned factors push towards the development of innovative modulation schemes for the future wireless technologies that can attain the best utilization of the limited radio spectrum available for communication purposes in an energy efficient way [6, 7].

Traditionally, orthogonal channels have been used to increase the number of users in wireless systems. According to this approach, multiple users do not only access multiple

channels in a flexible way, but throughput can also be improved significantly. Basically, to avoid mutual interference among users in multiple access channels, orthogonal channels are often established. The orthogonal characteristics can be obtained in different domains such as time, frequency, space, or code domains. Motivated by these characteristics, three main technologies, named as direct-sequence code-division multiple accesses (DS-CDMA), multiple-input multiple-output (MIMO), and orthogonal frequency division multiplexing (OFDM) have been proposed and become popular in many applications and standards.

In particular, in coherent [8] or non-coherent [9] spread spectrum schemes, orthogonal channels are created by using orthogonal codes to spread the data and support multiple users in the meanwhile.

Taking the advantages of the DS-CDMA, a modified scheme named as multi-carrier multi-code CDMA (MC-MC-CDMA) has been proposed to provide the multi-rate transmission capability for different users [10]. In the same vein, a new method is proposed in [11] using the parity bits to select a spreading sequence from a set of orthogonal spreading sequences. At the receiver side, the receiver detects which spreading code is employed then the data is recovered in the next step. Therefore, by applying this method, the coding gain is enhanced, the system is immunized against errors and the BER is further decreased. The same idea is extended later to MIMO-CDMA and multiuser scenarios to prove its feasibility [12–15]. On the other hand, OFDM is adopted in modern wireless systems to achieve orthogonal channels in the frequency domain. This modulation is mainly employed to combat frequency selective fading due to multipath propagation [16].

Another popular technology is MIMO system in which the transmitter and receiver are equipped with multiple antennas to capture the spatial diversity of scattering environments. According to this approach, complex techniques such as spatial multiplexing, diversity and beamforming can be applied to improve the reliability of communication and boost the data transmission rate. More specifically, the space-time block codes [17, 18] or space-time trellis codes (STTC) [19] can be applied for MIMO systems to enhance the bit error rate (BER) performance. Also, the beamforming can be implemented to steer the radiation pattern towards a certain direction, and the corresponding array gain can be used to improve the signal-to-noise ratios (SNRs) at the receiver [20–22].

Recently, a promising modulation technique has been developed aiming to increase the data rate and save the energy. This modulation known as spatial modulation (SM) uses multiple antennas at the transmitter side where just one antenna is

G. Kaddoum, Y. Nijsure and H. Tran are with University of Québec, ETS Engineering School, LACIME Laboratory, Montreal, Canada (e-mail: georges.kaddoum@etsmtl.ca).

Copyright (c) 2015 IEEE. Personal use of this material is permitted. However, permission to use this material for any other purposes must be obtained from the IEEE by sending a request to pubs-permissions@ieee.org.

activated at a time and its index is used as means to convey the information [23, 24]. Consequently, such technique can avoid inter-channel interference (ICI), antenna synchronisation and reduce the complexity of MIMO systems [25]. In [24], a more generalized spatial modulation (GSM) has been introduced in which more than one transmit antenna is activated in each time slot. The numerical results have illustrated that the bit rate grows considerably faster with the number of transmit antennas.

### Contributions and paper outline

Motivated by all aforementioned problems, in this paper, we propose a generalized code index modulation (CIM) for direct sequence-spread spectrum (DS-SS) communication. In this modulation, the information bits are mapped to the constellation symbols and the spreading code index. Furthermore, SM and CIM are two modulation schemes that belong to two different communication methods, however, they share the common goal of using an *index* as an additional parameter to convey information. The first uses multiple antennas at the transmitter side where just one antenna is activated at a time and its index is used as means to convey the information. The second uses multiple spreading codes, where a certain code is selected and its index is used as a mechanism to ferry the data.

The main contributions are summarized as follows:

- A generalization of the code index modulation (CIM) technique presented in [26] is proposed and analyzed.
- A spreading code index is used as an information-bearing unit to increase the data rate, to enhance the spectral and energy efficiency without adding extra hardware complexity to the system for moderate number of mapped bits.
- Analytical expressions for bit error rate (BER), symbol error rate (SER), throughput, system's complexity and energy efficiency are derived to evaluate the performance of the proposed system.
- The BER and SER performances of the CIM system are compared to a SS M-PSK modulation with the same number of bits per symbol to show the advantage of our approach.
- Additionally, these performance expressions are used to compare the CIM performance with SM scheme.

The remainder of this paper is organized as follows. In Section II, the generalized CIM system model and channel assumptions are described. In Section III, performance analysis in terms of BER and SER for the CIM system is provided. Complexity and energy consumption are analyzed in Section IV. Section V provides simulation results and performance comparison with conventional DS-SS and SM scheme. Finally, conclusions are discussed in section VI.

## II. SYSTEM MODEL

Consider a system model for the CIM as shown in Fig. 1 in which M-ary digital modulation with  $M$  symbols and DS-SS with  $2^N$  orthogonal Walsh codes  $\mathcal{W} = \{\mathbf{w}_1, \dots, \mathbf{w}_{2^N}\}$  are employed at the transmitter. Each spreading code consists of

$L$  chips with chip period  $T_c$  where the  $j^{\text{th}}$  code is represented in the vector form as  $\mathbf{w}_j = [w_{j,1}, \dots, w_{j,L}]^T$ . Here, M-ary phase-shift keying (M-PSK) is preferred in such scheme due to its low energy consumption as compared to other amplitude modulation techniques. Therefore, an M-QAM modulations can be used if energy is not a constraint and other orthogonal spreading codes may be applied. The information bits are arranged into blocks for transmission with  $N_t$  bits per block. The first sub-block with length  $2N$  bits is denoted as the mapped bits and the second sub-block with length  $n$  bits is denoted as the modulated bits. Thus, the total number of transmitted bits per block is given as  $N_t = 2N + n$ . The  $i^{\text{th}}$  block of bits is presented in vector form as  $\mathbf{d}_i = [d_{1,i}, \dots, d_{2N+n,i}]^T = [\mathbf{d}_{I,i}^T \mathbf{d}_{Q,i}^T \mathbf{d}_{M\text{-ary},i}^T]^T$  where  $\mathbf{d}_{M\text{-ary},i}$  is the modulated  $n$  bits sub-block which is modulated into the M-ary symbol  $s_i$  given by

$$s_i = a_i + jb_i. \quad (1)$$

where  $a_i$  and  $b_i$  are the real and imaginary components of the symbol  $s_i$ , respectively. The vectors  $\mathbf{d}_{I,i}$  and  $\mathbf{d}_{Q,i}$  have  $N$  bits each and constitute mapped sub-blocks. Note that each combination of mapped bits in the sub-block can generate a spreading code to spread the real and imaginary components of the M-ary symbol. Accordingly, the transmitted CIM signal  $y(t)$  can be expressed as

$$y(t) = \sum_{i=1}^B \sum_{k=1}^L \left\{ a_i w_{\mathbf{d}_{I,i},k} p(t - (iL + k)T_c) \cos(2\pi f_0 t) + b_i w_{\mathbf{d}_{Q,i},k} p(t - (iL + k)T_c) \sin(2\pi f_0 t) \right\}, \quad (2)$$

where  $B$  is the number of transmitted blocks,  $w_{\mathbf{d}_{I,i},k}$  and  $w_{\mathbf{d}_{Q,i},k} \in \mathcal{W}$  are the corresponding spreading sequences for the mapped bits vectors  $\mathbf{d}_{I,i}$  and  $\mathbf{d}_{Q,i}$ , respectively,  $j$  and  $j'$  represent the two indices of the selected spreading codes of  $2^N$  codes. In addition,  $L$  represents the spreading gain,  $f_0$  is the carrier frequency and  $p(t)$  is the pulse shaping filter which is a rectangular pulse of unit amplitude in  $[0, T_c]$ . Without loss of generality, the time chip  $T_c$  is considered to be equal to 1.

In the proposed scheme, the receiver has  $2^N$  correlators to process the in-phase signal and  $2^N$  correlators to manipulate the quadrature signal as seen in Fig. 1 (b). As the signal is transmitted to the receiver, it may be subject to fading effects due to randomness of wireless channels. As a result, the received signal over a fading channel is given as

$$r(t) = h(t) * y(t) + u(t), \quad (3)$$

where  $h(t)$  is the channel coefficient,  $*$  is the convolution operator and  $u(t)$  is a complex additive white Gaussian noise (AWGN) with zero mean and variance  $N_0$ . Furthermore, we assume that communication takes place over a Rayleigh quasi-static flat fading channel and that perfect channel state information is available at the receiver. After base-band signal recovery and sampling, the received sample signal is multiplied in parallel by the  $2^N$  Walsh codes. The  $2^N$  output signals are separated into in-phase and quadrature branches and summed over the bit duration  $LT_c$  in each branch to detect the spreading code. The code detection is performed

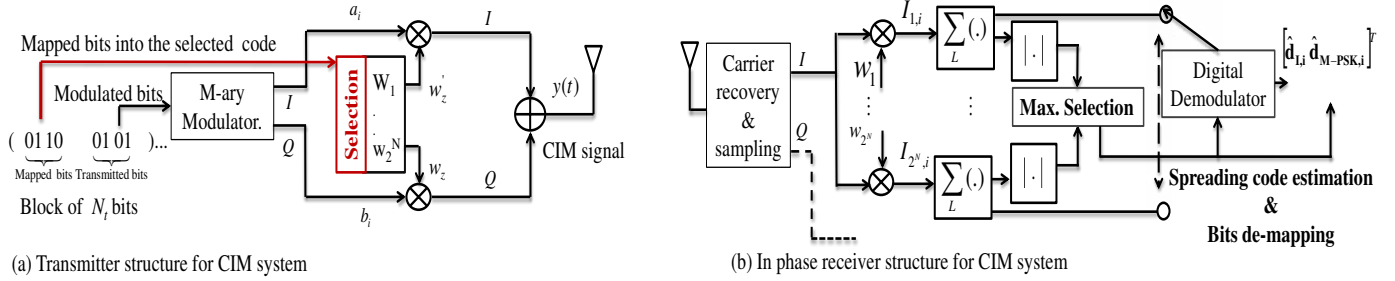


Fig. 1. System model

by selecting the maximum absolute value of the  $2^N$  correlator outputs. Once the code (i.e correlator output) is selected for in-phase and quadrature branches, the M-ary digital demodulator is performed to recover the transmitted symbol  $s_i$  of the  $i^{\text{th}}$  block.

Because the in-phase and quadrature components are of similar structure, we can focus the analysis on the in-phase branch  $I$  of the received signal given in equation (3) without loss of generality. Hence, after perfect carrier recovery, the base-band signal of the  $I$  component is expressed by

$$I(t) = \sum_{i=1}^B \sum_{k=1}^L h_i(t) a_i w_{\mathbf{a}_{I_{j,i},k}} p(t - (iL + k)T_c) + u_I(t), \quad (4)$$

where  $u_I(t)$  is the AWGN noise of the  $I$  component.

After channel compensation, the in-phase signal of equation (4) is multiplied in parallel by the  $2^N$  different Walsh codes and summed over symbol duration  $T = LT_c$ . Therefore, the output at the  $\hat{j}^{\text{th}}$  in-phase branch  $I_{\hat{j},i}$  of the  $i^{\text{th}}$  block can be expressed as

$$I_{\hat{j},i} = \sum_{k=1}^L (|h_i|^2 a_i w_{\mathbf{a}_{I_{j,i},k}} w_{\mathbf{a}_{I_{\hat{j},i},k}} + h_i w_{\mathbf{a}_{I_{j,i},k}} u_{I,\hat{j},i}) \quad (5)$$

and we can rewrite the equation (5) as follows:

$$I_{\hat{j},i} = \begin{cases} \pm \frac{|h_i|^2 E_s}{2} + v_{\hat{j},i} & \text{if } w_{\hat{j}} \text{ is transmitted (i.e } j = \hat{j}) \\ v_{I,\hat{j},i} & \text{if } w_{\hat{j}} \text{ is not transmitted (i.e } j \neq \hat{j}) \end{cases} \quad (6)$$

where  $E_s/2 = \sum_{k=1}^L w_{j,k}^2$  is the code energy for  $I$  component,  $v_{I,\hat{j},i} = \sum_{k=1}^L (h_i w_{\mathbf{a}_{I_{j,i},k}} u_{I,\hat{j},i})$  is correlated noise and  $h_i$  is the channel coefficient of the  $i^{\text{th}}$  block. The absolute values of the  $2^N$  correlator's outputs are compared in order to find the largest outcome and determine the corresponding transmitted Walsh code

$$\hat{j} = \arg \max_j \{|I_{j,i}|\}, \quad j \in \{1, \dots, 2^N\} \quad (7)$$

By estimating the index of the maximum correlator's output, the receiver knows which code is selected to spread the symbol, which allows to extract the  $N$  mapped bits per component. The quadrature component is detected in the same way. Once the code index detection is done, the receiver demodulate the corresponding correlator's output using an M-PSK demodulator. The performance of the proposed CIM system is investigated in the following section.

### III. PERFORMANCE ANALYSIS

In this section, we derive the BER and SER expressions, then we analyse the spectral efficiency and the throughput for the proposed CIM system.

#### A. BER analysis

According to the CIM system, we can see a fact that the total probability of BER, defined as  $P_T$ , is a function of the probability of BER for the modulated bits, denoted as  $P_{eb}$ , and the probability of BER for mapped bits, given as  $P_{em}$ . Moreover, in the in-phase branch, the probability of BER for mapped bits  $P_{em}$  is dependent upon the number of mapped bits  $N$ , and the probability associated with erroneous code detection is  $P_{ed}$ . Each combination may have different number of incorrect bits compared to the correct bit combination. For example, if the mapped bits are 0, 0, 0, the number of bit errors can be either one or three if the detected combination was 0, 0, 1 or 1, 1, 1 respectively. The probability of detecting one of the remaining  $2^N - 1$  incorrect combinations is the same for all codes and it equals to  $\frac{1}{2^N - 1}$ . Therefore, the probability of BER for the mapped bits can be formulated as

$$P_{em} = \frac{P_{ed}}{N(2^N - 1)} \sum_{c=1}^N \binom{N}{c} \quad (8)$$

where  $\binom{N}{c}$  represents the number of combinations having  $c$  bits different from the correct bit combination. As a result, the total probability of BER for the generalized CIM system is formulated as

$$P_T = \frac{n}{n + 2N} P_{eb} + \frac{2N}{n + 2N} P_{em} \quad (9)$$

where  $n + 2N$  is total number of transmitted bits in which  $n$  is the number of modulated bits while  $2N$  is the number of mapped bits. It is easy to see that the total probability of BER,  $P_T$ , is obtained only if the probability of BER for the mapped bits  $P_{em}$  and modulated bits  $P_{eb}$  are calculated. Here,  $P_{em}$  is already calculated in (8) and the probability of BER for the modulated bits  $P_{eb}$  is discussed as follows:

We can see that the correct reception of the modulated bits depends on the code detection and the M-ary modulation. The error may occur in two different cases. *Case 1*: there is no error in the spreading code detection (i.e no error in the mapped bits), but the modulated symbol is impossible to detect. *Case 2*: there is an error in the code detection (i.e error

in the mapped bits) and the modulated symbol is detected based on demodulation of incorrect selected correlator output. Consequently, the probability of BER for the modulated bits can be expressed as

$$P_{eb} = P_{ss} (1 - P_{em}) + \frac{1}{2} P_{em}, \quad (10)$$

where  $P_{ss}$  represents the probability of BER for the conventional SS M-ary system which depends on the number of modulated bits  $n$  and  $P_{em}$  is already calculated in (8). The theoretical expression of  $P_{ss}$  for the M-PSK can be found in [27, 28]. The factor  $\frac{1}{2}$  indicates a fact that with an error in the mapped bit detection  $P_{em}$ , the bit value detected based on the incorrect demodulated branch still matches the modulated bit half of the times. It is easy to see that (9) and (10) are computable as long as the error probability for spreading code detection  $P_{ed}$  is obtained.

### B. SER analysis

The SER of the CIM system is derived from the BER analysis of the previous section. In this system each symbol contains  $n$  modulated bits and  $2N$  mapped bits. Therefore, the total SER of this system  $SER_T$  is a function of the SER of the modulated symbols  $SER_{es}$  for a given M-ary modulation and the SER of the  $N$  mapped bits  $SER_{sm}$ . A total symbol error occurs either if an incorrect spreading code is chosen as a result of an incorrect estimation of the *mapped bits* or if a correct spreading code is chosen but the despreading operation results in an erroneous estimation of the *modulated bits*. Therefore, the  $SER_{sm}$  is the same as the probability of detecting incorrect code  $P_{ed}$  given in the BER analysis section

$$SER_T = SER_{es} + P_{ed}. \quad (11)$$

On the other hand, the  $SER_{es}$  of the modulated symbol occurs if the correct code is detected but an error occurs in the symbol demodulation

$$SER_{es} = SER_{ss} (1 - P_{ed}), \quad (12)$$

where  $SER_{ss}$  is the SER for the given conventional M-PSK which can be found in [27, 28]. Finally the total SER is given by

$$SER_T = SER_{ss} (1 - P_{ed}) + P_{ed}. \quad (13)$$

### C. Erroneous code detection probability $P_{ed}$

In this part, we will analyse the derivation of the erroneous code detection probability  $P_{ed}$  expression required to compute the BER and SER expressions. In order to estimate the transmitted spreading code index, the CIM receiver selects the maximum absolute value from the  $2^N$  values given at the output of the different branch. For equiprobable transmitted spreading codes, the error probability conditioned to the spreading code  $w_{\mathbf{a}_{I_{j,i}}}$  and a channel coefficient  $h_i$  is given

$$p_{ed} = \Pr \left( \left| I_{i,\hat{j}} \right| < \min_{\substack{j \in \{1,2,\dots,2^N-1\} \\ j \neq \hat{j}}} \left\{ |I_{i,j}| \right\} \middle| w_{\mathbf{a}_{I_{j,i}}}, h_i \right), \quad (14)$$

where  $I_{i,\hat{j}} = \frac{\pm E_s |h_i|^2}{2} + v_{I_{i,\hat{j}}}$  and  $I_{i,j} = v_{I_{i,j}}$ .

The  $2^N - 1$  random variables  $|I_{i,j}|$  are independent. In fact, each noise signal value of  $|I_{i,j}|$  is obtained by multiplying the AWGN samples by different spreading code and summed over a duration  $LT_c$ , this gives independent random values. The absolute of these Gaussian random values follows folded normal distribution [29]. Since the different random variables  $|I_{i,j}|$  are independents and following the folded normal distribution, then the order statistic theory can be applied to compute equation (14).

Therefore, to calculate the probability given in (14), let us consider the following lemma.

*Lemma 1:* Assuming that  $X = \min\{X_k\}$ ,  $k = 1 \dots K$  ( $K = 2^N - 1$ ), and  $Y = |I_{i,\hat{j}}|$  are random variables distributed following identical folded normal distribution in which the probability density function of  $Y$  and cumulative distribution function of  $X_k$  are formulated, respectively, as [29]

$$f_Y(y) = \frac{\sqrt{2}}{\sigma_Y \sqrt{2\pi}} e^{-\frac{(y-E\{Y\})^2}{2\sigma_Y^2}} + \frac{\sqrt{2}}{\sigma_Y \sqrt{2\pi}} e^{-\frac{(y+E\{Y\})^2}{2\sigma_Y^2}} \quad (15)$$

$$F_{X_k}(x) = \text{erf} \left( \frac{x}{\sqrt{2}\sigma} \right). \quad (16)$$

Accordingly, the probability of  $Y < X$  is calculated as follows:

*Proof:*

$$\Pr\{Y < X\} = \int_0^\infty \Pr\{y < X\} f_Y(y) dy \quad (17)$$

$$= \int_0^\infty \prod_{k=1}^K \Pr\{y < X_k\} f_Y(y) dy. \quad (18)$$

Therefore, the erroneous code detection probability for a given channel gain  $h_i$  can be expressed as

$$p_{ed} = \frac{1}{\sqrt{\pi\sigma_Y^2}} \int_0^\infty \left[ 1 - \text{erf} \left( \frac{y}{\sqrt{2}\sigma_Y} \right) \right]^K \left( e^{-\frac{(y-E\{Y\})^2}{2\sigma_Y^2}} + e^{-\frac{(y+E\{Y\})^2}{2\sigma_Y^2}} \right) dy. \quad (19)$$

We note that  $I_{i,\hat{j}}$  is a random variable distributed following normal distribution which has the mean and variance are  $|h_i|^2 E_s/2$  and  $|h_i|^4 E_s N_0/4$ , respectively. Accordingly, the mean and variance of the random variable  $Y = |I_{i,\hat{j}}|$  can be developed as [29]

$$E\{Y\} = \underbrace{\left( \sqrt{\frac{|h_i|^4 E_s N_0}{2\pi}} e^{-\frac{E_s}{2N_0}} - \frac{|h_i|^2 E_s}{2} \text{erf} \left( -\sqrt{\frac{E_s}{2N_0}} \right) \right)}_{=\beta} \left( \sqrt{\frac{E_s N_0}{2\pi}} e^{-\frac{E_s}{2N_0}} - \frac{E_s}{2} \text{erf} \left( -\sqrt{\frac{E_s}{2N_0}} \right) \right) |h_i|^2. \quad (20)$$

$$\sigma_Y^2 = \left( \frac{|h_i|^2 E_s}{2} \right)^2 + \frac{|h_i|^4 E_s N_0}{4} - E\{Y\}^2. \quad (21)$$

After some straightforward operations the variance of  $Y$  is obtained as

$$\sigma_Y^2 = \underbrace{\left( \frac{E_s}{4}(E_s + N_0) - \left( \sqrt{\frac{E_s N_0}{2\pi}} e^{-\frac{E_s}{2N_0}} - \frac{E_s}{2} \operatorname{erf}\left(-\sqrt{\frac{E_s}{2N_0}}\right) \right)^2 \right)}_{=\rho} |h_i|^4 \quad (22)$$

Hence, the probability  $p_{ed}$  is calculated as

$$p_{ed} = \frac{1}{|h_i|^2 \sqrt{\pi\rho}} \int_0^\infty \left[ 1 - \operatorname{erf}\left(\frac{y}{|h_i|^2 \sqrt{2\rho}}\right) \right]^K \left( e^{-\frac{(y-\beta|h_i|^2)^2}{2\rho|h_i|^4}} + e^{-\frac{(y+\beta|h_i|^2)^2}{2\rho|h_i|^4}} \right) dy \quad (23)$$

Finally, the average erroneous code detection probability over fading channel  $P_{ed}$  is equal to:

$$P_{ed} = \int_0^\infty \int_0^\infty p_{ed} f_h(\alpha) dy d\alpha \quad (24)$$

where  $f_h(\alpha)$  is the PDF of channel gain. To the best of authors's knowledge, the closed-form expression is not available. However, the above integral can be simplified easily by using popular computation software such as Mathematica or Matlab and leaving the numerical integration as solution to compute the erroneous code detection probability. ■

Finally, the total BER of the CIM-SS system subject to fading channel is obtained by substituting (24) and (10) into (9). For AWGN case, the channel coefficient is equal to one (i.e.  $h(t) = 1$ ). The closed-form expression of the error probability  $P_{ed}$  is obtained directly from (19) and the total BER under AWGN channel is achieved by substituting (19) for  $h = 1$  and (10) into (9).

#### D. Throughput analysis

In order to understand the enhancement behaviour of the CIM system we analyse its throughput. Typically, the throughput is defined as the number of correct bits (i.e bit level analysis) a user receives per unit time which can be written as [16]

$$R_t = Nt \frac{(1 - \text{BER})}{T}, \quad (25)$$

where  $Nt$  is the number of total transmitted bits per symbol in conventional or CIM modulations,  $T$  is the transmission time,  $BER$  is the bit error probability, and  $(1 - \text{BER})$  is the correct bits received during time  $T$ .

### IV. ENERGY EFFICIENCY AND COMPLEXITY

In this section, we evaluate the energy efficiency and system complexity of the generalized CIM system. We first show the energy saving achieved from mapping part of the transmitted bits into spreading codes. Then, we examine the effect of multiple spreading codes on the system complexity. Finally, we discuss the advantages and disadvantages of the CIM and SM techniques.

#### A. Energy efficiency

In the proposed CIM system, only  $n$  bits from the total transmitted  $N_t$  bits are directly modulated using the M-ary modulation while  $2N$  bits are conveyed in the spreading code selection. Considering that each modulated bit requires an energy of  $E_b$  to be transmitted, then mapping part of the  $N_t$  transmitted bits to the spreading codes reduces the total required transmission energy. Therefore, the percentage of energy saving in the CIM as compared to the conventional SS M-ary system for the same number of transmitted bits  $N_t$  can be stated as

$$E_e = \frac{2N}{n + 2N} \% \quad (26)$$

Clearly, an augmentation in the number of mapped bits  $2N$  results in more energy saving in the CIM system.

#### B. System complexity

The complexity improvement of the CIM scheme is evaluated here by the number of spreading/de-spreading operations required to transmit one symbol as compared to the conventional SS M-ary system. At the transmitter side, the CIM scheme requires two spreading operations to transmit one symbol which is the same number of operations required for the SS M-ary case. The only difference is that the CIM system uses two different spreading codes to perform the spreading operation for the in-phase and quadrature components rather than one spreading code for the two components as in the SS M-ary. At the receiver side,  $2 \times 2^N$  de-spreading/correlation operations are required for the in-phase and quadrature branches of the CIM system instead of two operations as in the SS M-ary system. However, while the CIM system requires just two spreading operations at the transmitter and  $2 \times 2^N$  de-spreading operations at the receiver to transmit  $N_t$  bits, the SS M-ary system requires  $2 + 2(2N/n)$  spreading operations and  $2 + 2(2N/n)$  de-spreading operations at the receiver side where  $2N/n$  represents the number of symbols corresponding to  $2N$  bits. Therefore, the total number of operation required for CIM system to transmit  $N_t$  bits is

$$\mathcal{O}_{\text{CIM}} = 2 + 2 \times 2^N, \quad (27)$$

and for SS M-PSK system it is

$$\mathcal{O}_{\text{M-PSK}} = 4 + 4 \times \frac{2N}{n}. \quad (28)$$

#### C. Comparison between CIM and SM

While both the CIM and SM are similar in using additional dimension to carry information bits, there are some advantages that make the CIM more attractive for practical implementation. The performance of the CIM depends on the orthogonality characteristics of the spreading codes rather than the channel characteristics. The performance of the SM degrades when the channels are correlated due to the inadequate spacing between antennas [30]. Using spreading codes rather than the antenna as an extra dimension for mapping bits moves the design challenge to finding spreading codes with good orthogonality characteristics. Moreover, the SM requires

multiple antennas at the transmitter, i.e., more cost is added to the hardware implementation. In addition, the number of mapped bits in the SM is limited by the physical size of wireless device where only small number of antennas can be used. On the other hand, we can use very large number of codes in the CIM by increasing the number of mapped bits without increasing the physical size and cost.

## V. NUMERICAL RESULTS

The objectives of this section are: to confirm the analytical performance expressions with the simulation results, to determine the number of modulated and mapped bits which achieves better performance and energy efficiency while keeping the system less complex, to show the trade-off between energy efficiency, system complexity, throughput, and error performance and finally, to compare the CIM to SM system.

### A. BER and SER performance

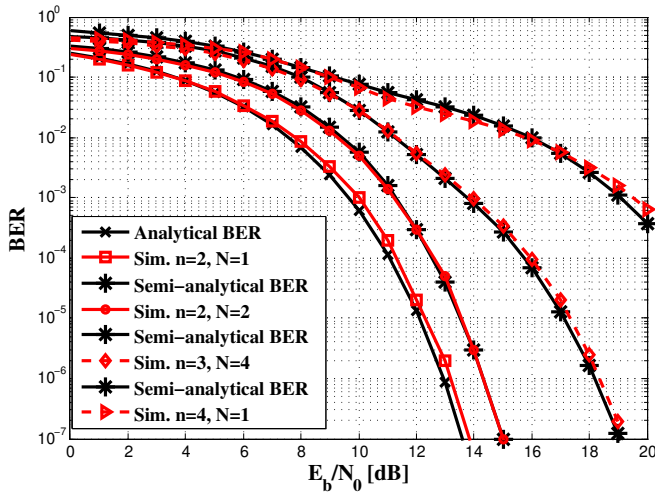


Fig. 2. Analytical BER and simulations for CIM system with M-PSK modulation for  $n = 2, 3, 4$ , and  $N = 1, 2, 4$  over an AWGN channel.

Fig. 2 shows the numerical semi-analytical (i.e semi-analytical because the integral of  $P_{ed}$  is computed numerically) BER expressions given in (9) for the CIM system under AWGN channel for different number of modulated and mapped bits and for a spreading gain of  $L = 64$ . As we can see from Fig. 2, the system performance degrades significantly as the number of modulated bits increases. This is due to the fact that the mapped bits do not affect the Euclidean distance of the M-PSK modulation. Also, we observe from Fig. 2 that the case of CIM system with  $n = 2$  and  $N = 2$  outperforms the case of  $n = 4$  and  $N = 1$ . The same behaviour can be observed from Fig. 3 and Fig. 4 for Rayleigh fading channel. This is because that the Euclidean distance of the former case is larger than the latter. This manifests an important remark that in CIM systems, it is better to increase the number of mapped bits and keep the Euclidean distance between symbols as large as possible. To better understand the degradation of performance with respect to the number of modulated and mapped bits,

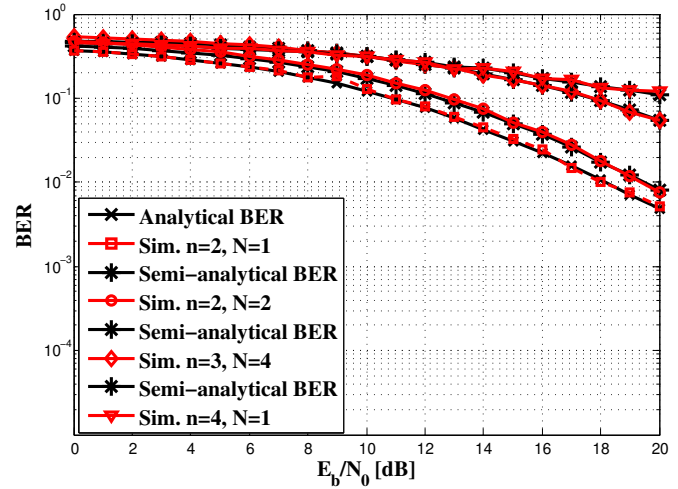


Fig. 3. Analytical BER and simulations for CIM system with M-PSK modulation for  $n = 2, 3, 4$ , and  $N = 1, 2, 4$  over Rayleigh fading channel with channel mean gain  $\mathbb{E}\{|h|^2\} = 0.5$ .

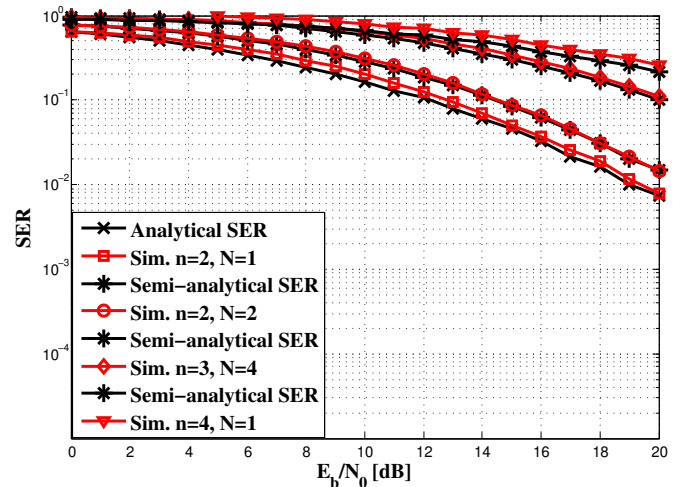


Fig. 4. Analytical SER and simulations for CIM system with M-PSK modulation for  $n = 2, 3, 4$ , and  $N = 1, 2, 4$  over Rayleigh fading channel with channel mean gain  $\mathbb{E}\{|h|^2\} = 0.5$ .

we simulate the BER for different number of modulated and mapped bits. As shown in Fig. 5, the best configuration in terms of error performance is using  $n = 2, N = 1$  and  $L = 64$ . As we increase the number of mapped bits, we can notice a gradual degradation in BER performance. On the other hand, the BER performance significantly degrades when the number of modulated bits is increased, because of the decrease in the Euclidean distance between the symbols. The advantage of our design as compared to the traditional digital modulations is when the proposed CIM system has the maximum Euclidean distance between the constellation symbols such as the case of  $n = 2$ , we can increase the number of transmitted bits by increasing the number of mapped bits  $N$  and still outperform the conventional SS M-PSK system with equivalent number of transmitted bits per symbol. Fig. 6 compares the throughput for the proposed CIM system with

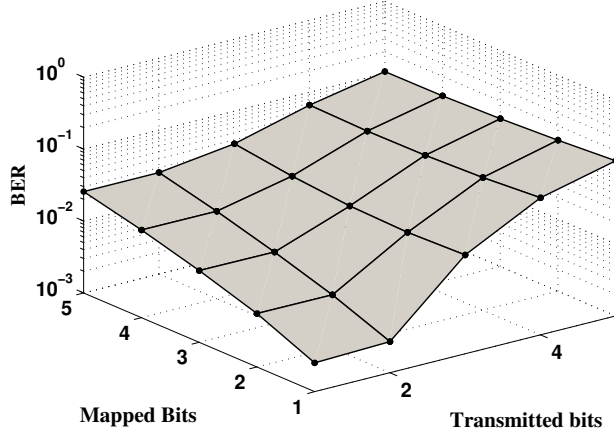


Fig. 5. BER for CIM at  $E_b/N_0 = 10$  dB.

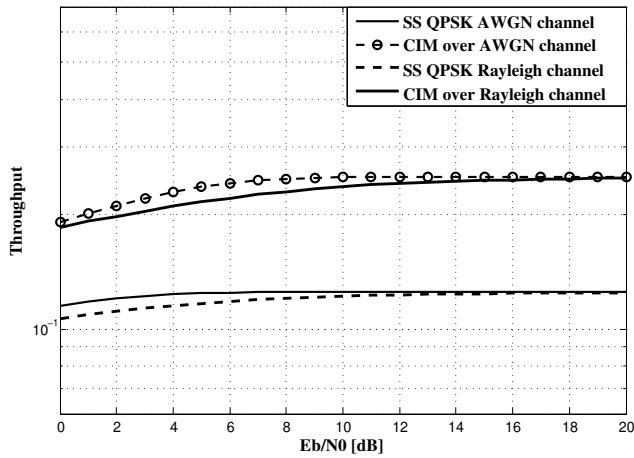


Fig. 6. Throughput of the CIM system modulation  $n = 2$ ,  $N = 1$  and SS-QPSK schemes over an AWGN and Rayleigh fading channels and spreading gain  $L = 16$ .

$n = 2$  and  $N = 1$  to the conventional SS-QPSK systems. Both SS-QPSK and CIM systems have the same bit duration  $T = LT_c$ . However, two bits are transmitted over  $T$  with SS-QPSK system while four bits are transmitted with CIM. As shown in Fig. 6, CIM offers a higher throughput than SS-QPSK. This is because in a given period  $T$ , CIM transmits four bits, two bits being physical transmissions and two bits being mapped to spreading codes. Consequently, the proposed system provides better spectral efficiency than the SS-QPSK system and saves half of transmission energy while being 25% less complex.

### B. Energy efficiency and complexity

Fig. 7 shows the complexity comparison of the CIM system given in (27) for  $n = 2$  and  $n = 3$  bits and different numbers of mapped bits  $N$  versus the SS M-PSK system given in (28) with equivalent number of transmitted bits. It is observed that

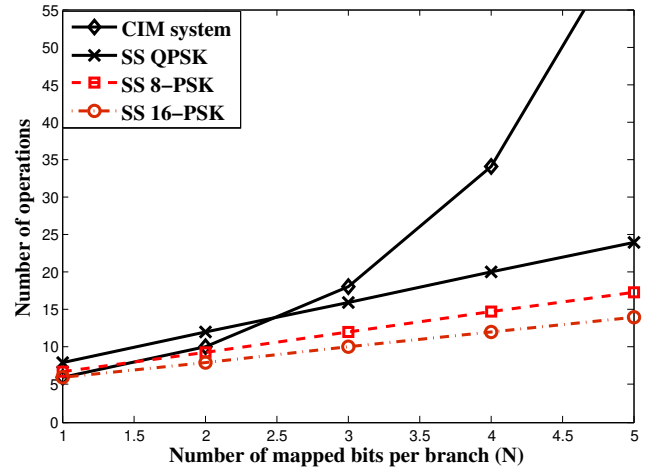


Fig. 7. Complexity comparison of the proposed CIM and conventional SS M-PSK systems.

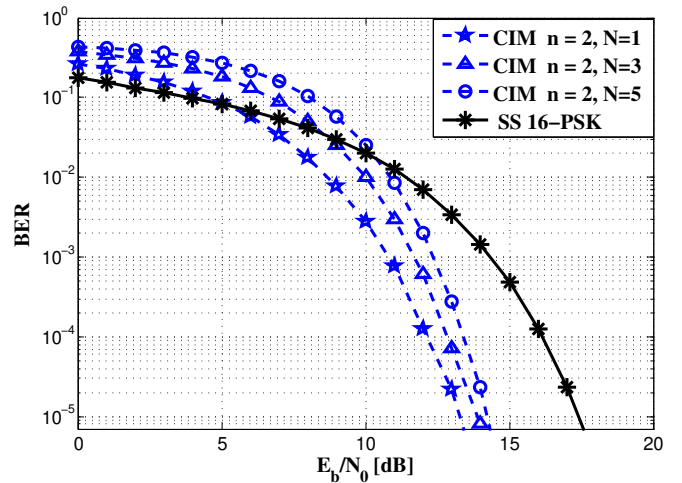


Fig. 8. BER performance comparison for CIM, and SS 16-PSK for AWGN channel and spreading gain  $L = 64$ .

for the same number of transmitted bits  $N_t$ , CIM starts to be more complex than the conventional SS M-PSK system when  $N > 2$ . Therefore, the number of mapped bits is restricted to  $N = 3$  bits at maximum such that complexity is kept close to that of the SS M-PSK. We consider the energy consumption given in (26) for the specific case of  $N = 1$ . With the configuration  $n = 2$  and  $N = 2$ , the CIM system achieves the transmission rate of SS 16-PSK (i.e.4 bits) while its complexity is 25% and its transmission power consumption is 50% less than SS QPSK.

### C. Special case of $n = 2$ and $N = 1, 2, 3$

Based on the aforementioned results of the complexity, energy efficiency and error performance, we conclude that the CIM system with  $n = 2$  and  $N \in \{1, 2, 3\}$  give an acceptable trade-off between complexity, energy efficiency, data rate and error performance. In this subsection, we show

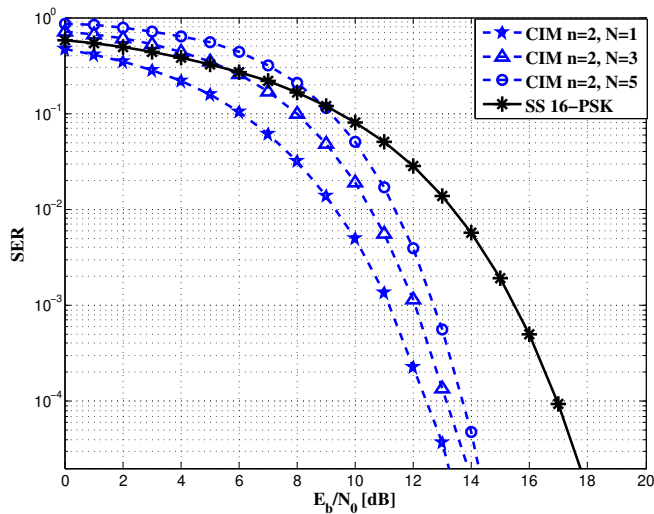


Fig. 9. SER performance comparison for CIM and SS 16-PSK for AWGN channel and spreading gain  $L = 64$ .

the BER and SER performance for these settings where the CIM is compared with the conventional SS M-PSK having an equivalent number of bits per symbol.

As shown in Figs. 8 and 9 (for the AWGN channel) and Figs. 10 and 11 (for the Rayleigh channel), the CIM system outperforms the conventional SS 16-PSK for the same number of bits per symbol and also for higher number of bits when the SNR is high. The SS 64-PSK and SS 256-PSK systems are not plotted in the same figure because the result is straightforward since the CIM already outperforms the SS 16-PSK. This performance gain can be attributed to the fact that our system provides larger Euclidean distance between the constellation symbols for the modulated bits. For the CIM, SS QPSK modulation is used and its Euclidean distance remains constant with increasing the number of mapped bits. This can explain the slow degradation in performance when the mapped bits are increased as compared to the conventional modulation in which the Euclidean distance decreases when the number of bits per symbol increases. In addition, as shown in Fig. 8 and Fig. 9, the performance of CIM-SS system even with  $N = 5$  outperforms the conventional system. However, when the number of mapped bits is more than  $N = 3$  the complexity of our systems grows rapidly making such system configuration impractical.

#### D. CIM and SM comparison

Here, we provide a comparison between our proposed CIM and the SM technique. In this comparison, we use SS-QPSK modulation for SM and compare it with CIM modulation for  $n = 2$  (i.e. SS-QPSK) with different number of mapped bits  $N \in \{1, 3, 5\}$  and for a spreading gain of  $L = 64$ . A Rayleigh fading channel with mean average powers of 0.5 is used for both systems. In addition, perfect knowledge of channel state information is assumed to be available at the receiver side for both systems. In this comparison, the SM uses four antennas at the transmitter side and one antenna at the receiver side while a single antenna is used in the CIM at

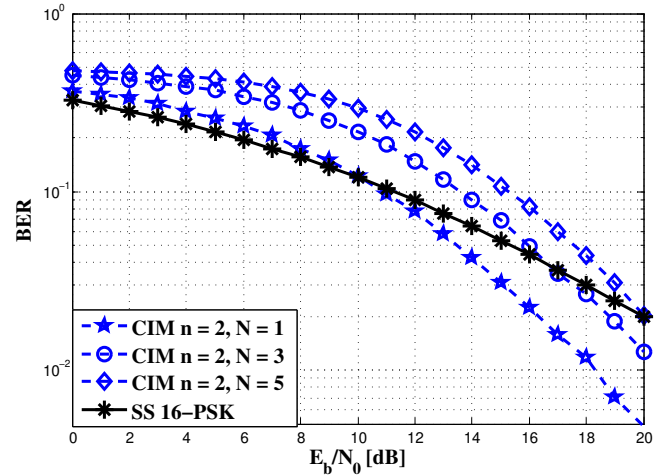


Fig. 10. BER performance comparison for CIM, SS 16-PSK for Rayleigh fading channel with channel mean gain  $E\{|h|^2\} = 0.5$  and spreading gain  $L = 64$ .

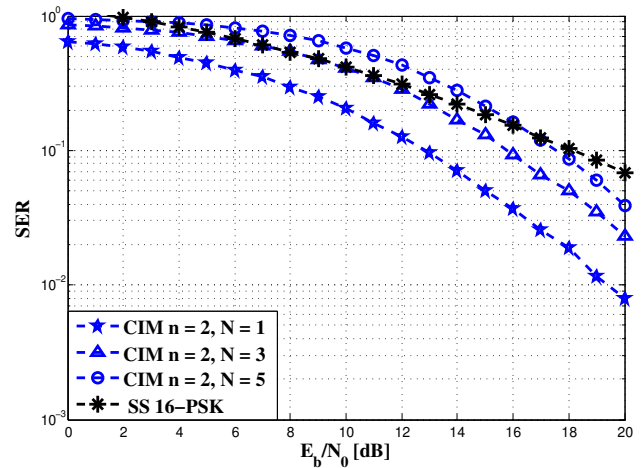


Fig. 11. SER performance comparison for CIM and SS 16-PSK for Rayleigh fading channel with channel mean gain  $E\{|h|^2\} = 0.5$  and spreading gain  $L = 64$ .

the transmitter and receiver sides. Maximum likelihood (ML) receiver is used for SM to estimate the transmit antenna index (number) and retrieve the corresponding mapped symbol. For the SM scenario, each received signal contains the modulated symbol and the mapped symbol corresponding to the active antenna which is equivalent to a CIM system with  $n = 2$  and  $N = 1$  in terms of transmitted bits. Fig. 12 plots the performance of these systems for flat fading channel. Fig. 12 shows that the proposed CIM system outperforms the SM system in BER performance. In addition we can see that for  $N = 3$ , CIM achieves 8 bits per transmission with lower complexity while SM achieves only 4 bits under a similar configuration.

## VI. CONCLUSION

In this paper, a new high data rate and energy efficient CIM system has been proposed. This system is based on an original idea to increase the data rate by using a new



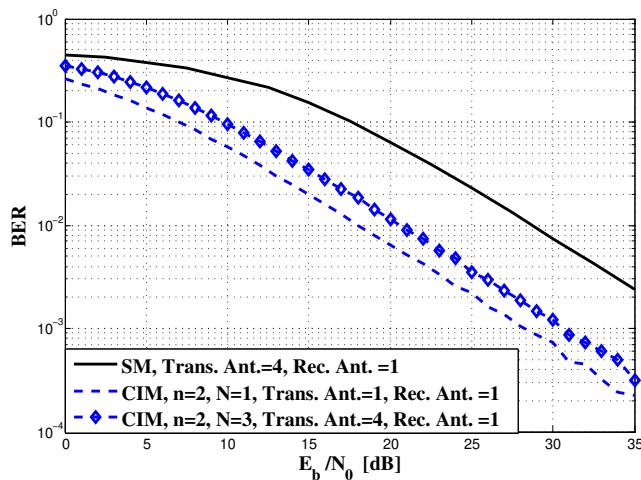


Fig. 12. Performance comparison of the proposed CIM and the SM systems.

dimension (the spreading code *index*) to map the information bits. General BER and SER expressions have been derived to evaluate the system performance. Simulation results confirm the corresponding theoretical expressions used in the analysis. Moreover, the spectral efficiency, throughput, energy efficiency, complexity, and error performance of the proposed system are analyzed and compared to the conventional DS-SS system. The numerical results for the proposed CIM system have illustrated an important remark that the choice of two modulated bits  $n = 2$  and less than three mapped bits for the in-phase and quadrature components  $N \leq 3$  achieves good BER performance with acceptable energy efficiency and complexity. In addition, we show that for  $n = 2$  and  $N = 1$ , the CIM model can save 50% of the transmitted energy and outperform the equivalent SS 16-PSK having the same number of bits per symbol while being 25% less complex as compared to the conventional SS QPSK system. In addition, the results reveal that our system outperforms the SM system in terms of the BER even when our system transmits 8 bits per symbol instead of 4 bits for the SM system. Since any enhancement in CIM system performance passes through improving detection algorithms and proposing new error coding methods profiting from the spreading code index, our future work will focus on this area to enhance the total BER performance over fading channels and to integrate this scheme with SM and MIMO systems.

#### ACKNOWLEDGEMENTS

This research has been supported by Natural Sciences and Engineering Research Council (NSERC) discovery grant 435243 – 2013 Canada.

#### REFERENCES

[1] R. Cavallari, F. Martelli, R. Rosini, C. Buratti, and R. Verdone, "A survey on wireless body area networks: Technologies and design challenges," *IEEE Communications Surveys Tutorials*, vol. 16, no. 3, pp. 1635 – 1657, Third Quarter 2014.  
 [2] I. Akyildiz, W. Su, Y. Sankarasubramaniam, and E. Cayirci, "A survey on sensor networks," *IEEE Communications Magazine*, vol. 40, no. 8, pp. 102–114, Aug. 2002.

[3] L. Atzori, A. Iera, and G. Morabito, "The internet of things: A survey," *Computer Networks*, vol. 54, no. 15, pp. 2787 – 2805, 2010.  
 [4] F. Alagoz and G. Gur, "Energy efficiency and satellite networking: A holistic overview," *Proceedings of the IEEE*, vol. 99, no. 11, pp. 1954–1979, Nov. 2011.  
 [5] P. Arapoglou, K. Liolis, M. Bertinelli, A. Panagopoulos, P. Cottis, and R. De Gaudenzi, "MIMO over satellite: A review," *IEEE Communications Surveys and Tutorials*, vol. 13, no. 1, pp. 27–51, First 2011.  
 [6] R. Baldemair, E. Dahlman, G. Fodor, G. Mildh, S. Parkvall, Y. Selen, H. Tullberg, and K. Balachandran, "Evolving wireless communications: Addressing the challenges and expectations of the future," *IEEE Vehicular Technology Magazine*, vol. 8, no. 1, pp. 24–30, Mar. 2013.  
 [7] G. Li, Z. Xu, C. Xiong, C. Yang, S. Zhang, Y. Chen, and S. Xu, "Energy-efficient wireless communications: Tutorial, survey, and open issues," *IEEE Transactions on Wireless Communication*, vol. 18, no. 6, pp. 28–35, Dec. 2011.  
 [8] S. Moshavi, "Multi-user detection for DS-CDMA communications," *IEEE Communications Magazine*, vol. 34, no. 10, pp. 124–136, Oct. 1996.  
 [9] Y. Lyu, L. Wang, G. Cai, and G. Chen, "Iterative receiver for M-ary DCSK systems," *IEEE Trans. on Communications*, vol. PP, no. 99, pp. 1–0, 2015.  
 [10] C. Lin I, G. Pollini, L. Ozarow, and R. Gitlin, "Performance of multi-code CDMA wireless personal communications networks," in *Proc. IEEE Vehicular Technology Conference*, vol. 2, Chicago, U.S.A, Jul. 1995, pp. 907–911.  
 [11] C. D'Amours, "Parity bit selected spreading sequences: a block coding approach to spread spectrum," *IEEE Communications Letters*, vol. 9, no. 1, pp. 16–18, Jan 2005.  
 [12] C. D'Amours and J.-Y. Chouinard, "Parity bit selected and permutation spreading for CDMA/MIMO systems in frequency-nonselective rayleigh fading channels," in *IEEE 65th Vehicular Technology Conference, VTC2007-Spring*, April 2007, pp. 1475–1479.  
 [13] C. D'Amours and A. Dahmane, "Permutation spreading for asynchronous MIMO-CDMA systems using Hadamard Codes and Gold scrambling sequences," in *IEEE Wireless Communications and Networking Conference, WCNC 2009*, April 2009, pp. 1–6.  
 [14] M. Shi, C. D'Amours, and A. Yongacoglu, "Design of spreading permutations for MIMO-CDMA based on space-time block codes," *IEEE Communications Letters*, vol. 14, no. 1, pp. 36–38, January 2010.  
 [15] A. Mirzaee and C. D'Amours, "Turbo receiver for MIMO-CDMA systems employing parity bit selected and permutation spreading," *EURASIP Journal on Wireless Communications and Networking*, vol. 2013, no. 1, 2013.  
 [16] D. Tse and P. Viswanath, *Fundamentals of wireless communication*. Cambridge university press, 2005.  
 [17] S. Alamouti, "A simple transmit diversity technique for wireless communications," *IEEE Journal on Selected Areas in Communications*, vol. 16, no. 8, pp. 1451–1458, Oct. 1998.  
 [18] V. Tarokh, H. Jafarkhani, and A. Calderbank, "Space-time block codes from orthogonal designs," *IEEE Transactions on Information Theory*, vol. 45, no. 5, pp. 1456–1467, Jul. 1999.  
 [19] V. Tarokh, N. Seshadri, and A. Calderbank, "Space-time codes for high data rate wireless communication: performance criterion and code construction," *IEEE Transactions on Information Theory*, vol. 44, no. 2, pp. 744–765, Mar. 1998.  
 [20] J. Mietzner and P. Hoeher, "Boosting the performance of wireless communication systems: theory and practice of multiple-antenna techniques," *IEEE Communications Magazine*, vol. 42, no. 10, pp. 40–47, Oct. 2004.  
 [21] A. Paulraj, D. Gore, R. Nabar, and H. Bolcskei, "An overview of MIMO communications - a key to gigabit wireless," *Proceedings of the IEEE*, vol. 92, no. 2, pp. 198–218, Feb. 2004.  
 [22] D. Gesbert, M. Shafi, D. shan Shiu, P. Smith, and A. Naguib, "From theory to practice: An overview of MIMO space-time coded wireless systems," *IEEE Journal on Selected Areas in Communications*, vol. 21, no. 3, pp. 281–302, Apr. 2003.  
 [23] M. Di Renzo, H. Haas, A. Ghayeb, S. Sugiura, and L. Hanzo, "Spatial modulation for generalized MIMO: Challenges, opportunities, and implementation," *Proceedings of the IEEE*, vol. 102, no. 1, pp. 56–103, Jan. 2014.  
 [24] Y. Xiao, Z. Yang, L. Dan, P. Yang, L. Yin, and W. Xiang, "Low-complexity signal detection for generalized spatial modulation," *IEEE Communications Letters*, vol. 18, no. 3, pp. 403–406, Mar. 2014.  
 [25] R. Mesleh, H. Haas, S. Sinanovic, C. W. Ahn, and S. Yun, "Spatial modulation," *IEEE Trans. on Vehicular Technology*, vol. 57, no. 4, pp. 2228–2241, July 2008.

- [26] G. Kaddoum, M. Ahmed, and Y. Nijsure, "Code index modulation: A high data rate and energy efficient communication system," *IEEE Communications Letters*, vol. 19, no. 2, pp. 175–178, Feb 2015.
- [27] J. Proakis, *Digital Communications*. McGraw-Hill, 2001.
- [28] M. K. Simon and M. S. Alouini, *Digital Communication over Fading Channels: A Unified Approach to Performance Analysis*, 2nd ed. New York: Wiley, 2000.
- [29] A. Papoulis, *Probability, random variables, and stochastic processes*. McGraw-Hill, 1991.
- [30] J. Wang, S. Jia, and J. Song, "Generalised spatial modulation system with multiple active transmit antennas and low complexity detection scheme," *IEEE Transactions on Wireless Communications*, vol. 11, no. 4, pp. 1605 – 1615, Apr. 2012.



**Georges Kaddoum** (M'11) received the Bachelor's degree in electrical engineering from the École Nationale Supérieure de Techniques Avancées (ENSTA Bretagne), Brest, France, and the M.S. degree in telecommunications and signal processing (circuits, systems, and signal processing) from the Université de Bretagne Occidentale and Telecom Bretagne(ENSTB), Brest, in 2005 and the Ph.D. degree (with honors) in signal processing and telecommunications from the National Institute of Applied Sciences (INSA), University of Toulouse, Toulouse,

France, in 2009. Since november 2013, he is an Assistant Professor of electrical engineering with the École de Technologie Supérieure (ETS), University of Quebec, Montréal, QC, Canada. In 2014, he was awarded the ETS Research Chair in physical-layer security for wireless networks. Since 2010, he has been a Scientific Consultant in the field of space and wireless telecommunications for several companies (Intelcan Techno-Systems, MDA Corporation, and Radio-IP companies). He has published over 70 journal and conference papers and has two pending patents. His recent research activities cover wireless communication systems, chaotic modulations, secure transmissions, and space communications and navigation. Dr. Kaddoum received the Best Paper Award at the 2014 IEEE International Conference on Wireless and Mobile Computing, Networking, and Communications, with three coauthors, and the 2015 IEEE Transactions on Communications Top Reviewer Award.



**Yogesh Nijsure** (M'12) received the B.E. degree (Distinction) in Electronics Engineering from University of Mumbai, India, in June 2006 and received his M.Sc. degree (Distinction) in Wireless Communication Systems Engineering from the University of Greenwich, U.K. in September 2008. He received his Ph.D. degree from University of Newcastle upon Tyne in U.K. in October 2012. From March 2010 to September 2010 he undertook his research internship at the Institute for Infocomm Research (I2R), Singapore, as a research engineer. From November 2011 to November 2012 he worked as a research associate at Nanyang Technological University, Singapore. From December 2012 to April 2014 he worked at Rockwell Collins India Pvt. Ltd. as a Technical Specialist Systems within the aerospace and defense research domain. Since May 2014, he is working as a post-doctoral research fellow at École de Technologie Supérieure (ETS), University of Quebec, Montreal, QC, Canada. He is a member of IEEE and has authored several Top-Tier IEEE conferences and IEEE Transaction journal publications. Till date he has submitted two patent applications in U.S.A and India respectively. His research interests include cognitive radar network design, Bayesian non-parametric methods for wireless sensor network applications, UWB radar systems, cognitive radio networks, wireless communication theory, information theory and radar signal processing, electronic warfare and software defined radio systems.



**Hung Tran** (M'12) was born in Hanoi, Vietnam, in 1980. He received the B.S. and M.S. degree in information technology from Vietnam National University, Hanoi, in 2002 and 2006, respectively, and the Ph.D. degree from Blekinge Institute of Technology, Karlskrona, Sweden, in March 2013. He is currently a Researcher with the Network Systems Section, Department of Information Technology, National Institute of Education Management, Hanoi. His research interests are in the areas of wireless communications, cognitive radio networks, and green cooperative communication systems.